Technical Note: Microstructural Evolution During Inertia Friction Welding of Austenitic Stainless Steels

BY J. C. LIPPOLD AND B. C. ODEGARD

Introduction

Inertia friction welding is a solid-state welding process, which utilizes the frictional heat generated between a rotating and a stationary workpiece to produce a metallurgical bond. Little or no melting occurs along the weld interface and this makes the process extremely attractive where difficult-to-weld or dissimilar metals are to be welded. The likelihood of solidification discontinuities is minimized or completely eliminated. Other advantages of inertia friction welding include reduced development and fabrication time, lower cost, and increased reproducibility. In addition, in similar metal welds the joint preparation is minimal because the process is essentially "self-cleaning"; the metal flow directed radially outward along the weld interface removes any contaminants associated with the initial faying surfaces.

Despite its advantages, inertia friction welding has not been widely accepted as a viable replacement for fusion welding. It is instead, viewed as a "last-ditch-effort" process which is used only when conventional methods fail. This may be due in part to the requirement for symmetry of the rotating member. However, many conventionally welded joints are, in fact, symmetric and capable of being inertia friction welded.

Although several review articles have addressed the process variables and associated temperature distribution during inertia friction welding (Refs. 1-5), the metallurgy of the process has received little attention. If inertia friction welding is to gain wider use as a replacement for fusion welding, the metallurgical response of materials during inertia friction welding must be better understood.

This report focuses on the characteristics of metal flow, localized heating, and associated microstructural changes which occur during the inertia friction welding of 300-series stainless steels. Future publications are expected to report the effects of composition, microstructure, and welding variables on the strength and fracture behavior of a variety of inertia friction welded austenitic stainless steels.

J. C. LIPPOLD and B. C. ODEGARD are with Sandia National Laboratories, Livermore, California.

Experimental Procedure

A free-machining grade of austenitic stainless steel — Type 303S — was selected to study the microstructural response of austenitic stainless steels during inertia friction welding. The selection of this alloy was based on several considerations:

1. The as-received material is heavily banded and contains sulfide stringers along these bands. Since the sulfide particles are relatively stable to almost the melting point of the alloy, they form a "fingerprint" of the metal flow which occurs during welding.
2. With the exception of the sulfur content, the composition of Type 303S stainless steel is equivalent to that of Type 304, a commonly used commercial stainless steel.
3. The alloy is normally unweldable using fusion welding techniques. It was of interest to determine if Type 303S stainless steel could be joined by inertia friction welding.

The (wt.-%) chemical composition of the alloy is 18.25 Cr, 9.03 Ni, 1.70 Mn, 0.56 Si, 0.04 C, 0.03 N, 0.02 P, and 0.17 S. Weld blanks 5.08 cm (2.0 in.) long and 1.27 cm (0.5 in.) in diameter were cut from 1.27 cm (0.5 in.) bar stock. The blanks were machined such that the faying surfaces were perpendicular to the specimen axis with a surface finish of 32 μ in or better.

The welding conditions are summarized in Table 1. Samples were cleaned in acetone prior to welding in order to remove any residual machining lubricants. The specimen pairs were measured prior to welding and again following welding in order to determine the total axial upset.

Following welding, representative samples were sectioned axially and metallographically prepared. A mixed acid etchant containing equal parts of nitric, hydrochloric, and acetic acid was used to reveal microstructural details.

Mechanical Testing

Smooth and notched tensile samples were machined from the welded blanks. The diameter of the smooth bar gage section was 4.95 mm (0.195 in). Two notch depths were used, including 1.23 mm (0.048 in.) and 0.825 mm (0.032 in.).

This procedure made it possible to measure weld strength as a function of radial distance from the center of the welded blanks. The strength may not be uniform, since the surface velocity decreases to zero at the axis of rotation. The tensile samples were tested at a crosshead velocity of 0.02 mm/s (0.05 ipm).

Table 1—Inertia Friction Welding Conditions[a]

Spindle moment of inertia:	1.5 $lb_m{}^{-ft^2}$ (6.32×10^{-2} kg · m^2)
Spindle rotational speed:	6600 RPM
Axial force:	6000 lb_f (26.4 kN)
Energy:[b]	81.94 kJ/in.^{2} (1.27 J/m^2)
Average axial upset:	0.142 in. (3.61 mm)

[a] E_T (kJ/in.^{2}) $= \frac{(\text{RPM})^2 \text{ (moment of inertia)}}{4332 \text{ (cross sectional area)}}$

Results

Optical Metallography

The inertia friction welding process for solid bars results in extensive metal flow radially outward along the weld interface. The photomacrograph shown in Fig. 1 reveals the nature of this flow near the axis of the Type 303S weld. Note that the flow lines, as delineated by the banding in the base metal, bend sharply in the vicinity of the weld interface.

The rapid change in flow direction suggests that the temperature gradient in this region is relatively steep. As a result the elevated temperature regime in which plasticity occurs is narrow and effectively limits plastic flow to a narrow band in close proximity to the weld interface. Within that region flow occurs radially outward parallel to the weld interface resulting in the realignment of intermetallic stringers perpendicular to the original base metal orientation.

At higher magnification (Fig. 2), the sulfide particles appear refined and homogeneous in contrast to the base metal structure. The combination of high temperature and plastic flow causes the elongated stringers (Fig. 2A) to fracture and partially dissolve, thus forming the low aspect ratio particles in the weld region (Fig. 2B). At the weld interface it is likely that the sulfides melt and act as a "lubricant" on the faying surfaces.

No metallographic evidence of sulfide melting was observed. However, the small amount of external flash produced at the outside diameter of the weld suggests that the presence of liquid films during welding reduced the amount of energy dissipated in the form of frictional heating at the mating surfaces.

A microhardness traverse across the weld region at a position midway between the center of the bar and the external surface (half-radius position) is shown in Fig. 3. The hardness drops steeply in the region of the weld where metal flow is significant. Near the center of the weld the hardness flattens out, corresponding to the homogeneous microstructural region shown previously in Fig. 2A. The hardness peak located precisely at the weld interface results from localized deformation which occurs during the final stages of the welding process. The nature of this deformation is discussed elsewhere in this report.

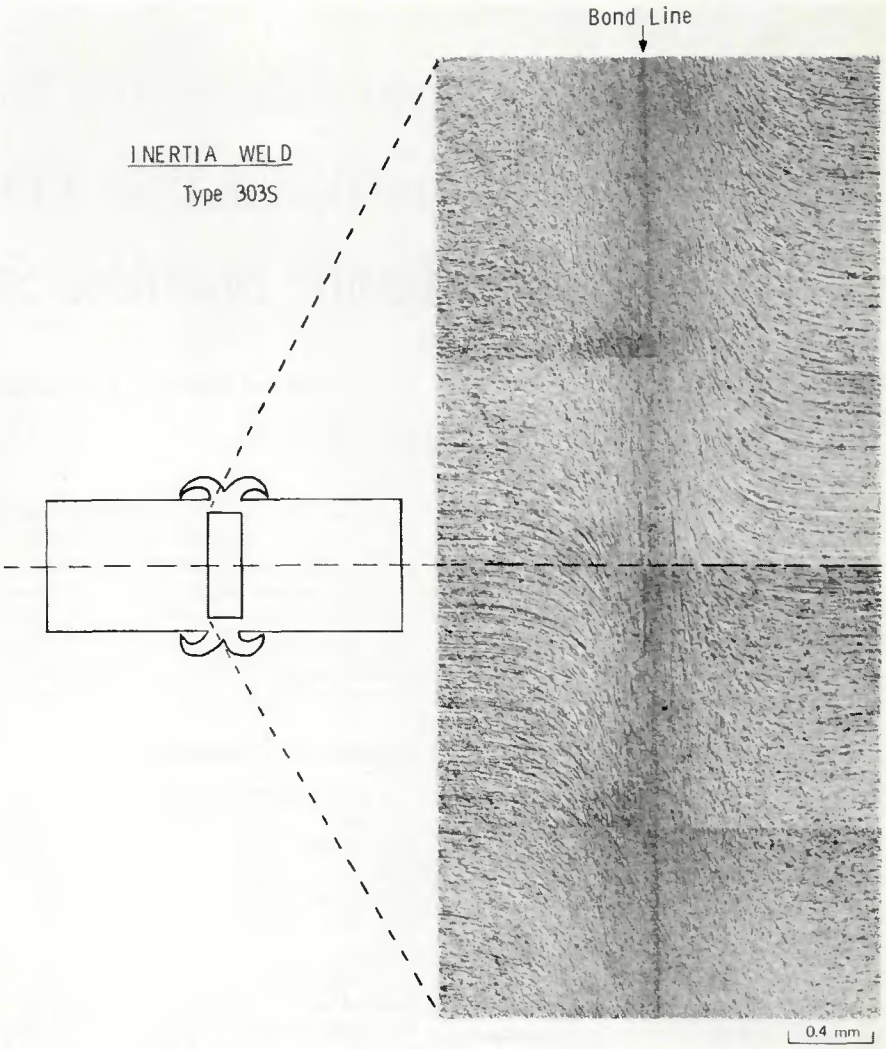

Fig. 1 — Macrostructure along the weld interface of an inertia friction weld in a solid bar of Type 303S stainless steel. Note the rapid change in stringer orientation close to the weld interface

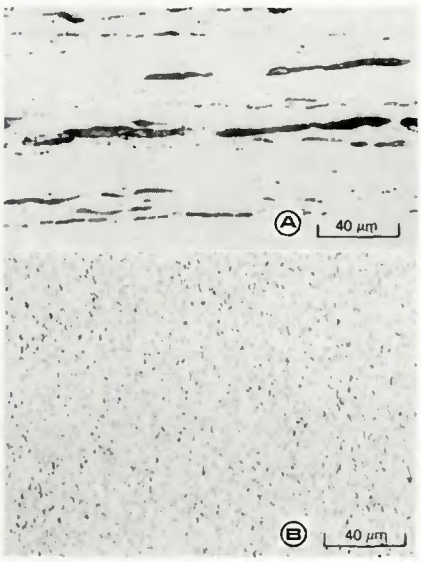

Fig. 2 — Sulfide morphology in: A — base metal; B — weld region

Tensile Test Results

The results of both smooth bar and notched bar tensile tests are summarized in Table 2. Failure in the smooth gage tensile bars of 303S occurred at the weld interface after minimal elongation. Further, the notched samples exhibited almost no ductility and only a moderate increase in tensile strength above the smooth bars. By comparison, reference samples of Type 304L stainless steel have exhibited notched-to-smooth strength ratios of 1.6 and 2.1 for the shallow and deep notch, respectively (Ref. 6).

These results indicate that there is little change in weld strength as a function of radial distance from the rotational axis.

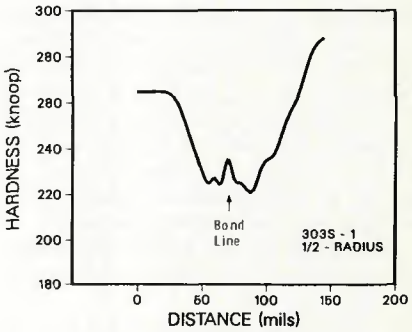

Fig. 3 — Hardness profile parallel to specimen axis midway between the rotational axis of the bar and the outside surface

Fig. 4 — Fracture surface of smooth bar tensile sample: A — low magnification showing spiral pattern; B — high magnification revealing "woody" fracture morphology

Table 2—Tensile Test Results[a], [b]

	YS, ksi(MPa)	UTS, ksi(MPa)	Elong, %	UTS_N/UTS_S
Smooth bar				
303S	60.0 (414)	95.3 (657)	4.6	–
304L	41.8 (288)	88.3 (609)	50	–
Notch A[c]				
303S	–	103.4 (713)	0.5	1.08
304L	–	142.1 (980)	9.5	1.61
Notch B[d]				
303S	–	121.3 (836)	0.4	1.27
304L	–	189.3 (1305)	2.2	2.14

[a]All values average of at least two tests.
[b]YS — yield strength; UTS — ultimate tensile strength; Elong — elongation.
[c]Cross section = 0.0133 in.^{2} (8.58 mm^2).
[d]Cross section = 0.0075 in.^{2} (4.84 mm^2).

Fracture Morphology

A low magnification SEM fractograph of the smooth bar fracture surface is shown in Fig. 4A. A distinct spiral pattern is evident emanating from the center of the bar. At higher magnification (Fig. 4B), the fracture surface appears to exhibit a "woody" morphology with no evidence of the discrete sulfide particles observed metallographically along the weld interface (Fig. 2).

Closer examination at ×6000 reveals the presence of the sulfide inclusions. The fractograph in Fig. 5A shows that the sulfides are present as thin, lenticular particles superimposed on the fracture surface.

In many cases, the particles were fractured (arrows in Fig. 5A), probably during the tensile test. The EDS spectrum in Fig. 5B, collected at a point corresponding to one of these particles, indicates that the particles are probably manganese-rich sulfides. (Since the Cr K_β peak overlies the Mn K_α peak, CrK_β peak is much higher than normal due to Mn enrichment of the particle.)

Discussion

The banded structure of Type 303S free-machining stainless steel provides a unique opportunity to study the nature of metal flow and microstructural development during inertia friction welding. By evaluating both metallographic cross sections parallel to the specimen axis and fracture surfaces along the weld interface, it is possible to construct a three-dimensional picture of the weld interface microstructural evolution.

From Fig. 1 it can be seen that near the center of the bar the region of metal flow is confined to a narrow band adjacent to the weld interface. Proceeding radially outward from the specimen center the region of plastic flow gradually broadens and eventually merges with the weld expulsion. The expulsion represents the metal which has been extruded from the joint. Since the temperature gradient along the axis varies as a function of position along the interface (Refs. 6-8) (that gradient being greater near the center than the outside surface), the width of the region in which metal flow occurs will increase proportionally upon moving radially outward from the center.

The hardness drop along the weld interface, shown in Fig. 3, is also a result of the temperature excursion in the vicinity of the weld interface. The hardness behavior mirrors the onset of metal flow; the hardness "trough" is narrowest at the center of the bar and widest near the outside diameter. In addition, the hardness gradient is the steepest at the center, corresponding to the region where the temperature gradient is the greatest and the metal flow is essentially zero. The softening results from the recovery and recrystallization that occurs at sub-solidus temperatures. This softening is mitigated to some extent by the work hardening promoted by the localized metal flow.

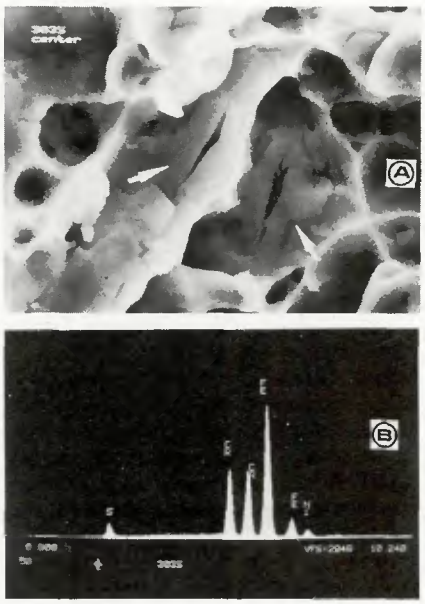

Fig. 5 — Sulfide particles on fracture surface: A — thin lenticular particles exhibiting secondary cracking; B — EDS spectrum from one of these particles (dark arrows)

The slight rise in hardness located at the weld interface in Fig. 3 results from deformation associated with the final revolution of the flywheel. The majority of metal flow occurs while the parts are spinning against each other; however, as the relative velocity drops the parts form a metallurgical bond and the remaining flywheel energy is dissipated as localized deformation along the weld interface.

The spiral pattern on the weld fracture surface in Fig. 4A provides a "fingerprint" of the metal flow which occurs in and near the plane of the weld. Since one part is spinning against the mating stationary part, metal flow is not simply radially outward; it is also rotational about the center of the specimen while flowing gradually toward the outside diameter. The flow pattern in inertia friction welds is geometry dependent; the spiral pattern observed in Fig. 4A can be expected when welding solid bars since metal cannot flow toward the center. When annular samples are welded, for example, metal flow will occur towards both the inside and outside diameter and the spiral pattern would not be formed.

The severe plastic deformation which occurs along the weld interface also has an effect on the aligned stringers. As the metal turns and flows in the plane of the weld interface, intermetallic particles making up the stringers are swept along and subjected to high temperatures and triaxial stresses. As a result of this thermomechanical processing, the particles are broken up and deformed in the weld region. The original sulfide stringers

shown in Fig. 2B are squeezed flat and form the thin lenticular particles observed on the fracture surface in Fig. 5. Since metal flow and, hence, particle motion along the weld interface is perpendicular to the specimen axis, the sulfides become aligned in an orientation transverse to the tensile axis. The combination of particle shape, orientation, and the brittle nature of the sulfide results in preferential failure at these sites and provides the "fingerprint" of the metal flow pattern observed in Fig. 4A. Such particles can and in this case did influence the strength of the weld.

Despite the inferior strength and ductility of the Type 303S stainless steel inertia friction weld, it was possible to produce a metallurgical bond which was essentially free of discontinuities.

Summary

A heavily banded Type 303S free-machining stainless steel has been used to reveal the pattern of metal flow during the inertia friction welding of solid bars. Deformation is restricted to a narrow band along the weld interface whose width is dictated by the local temperature gradient in that region. Recovery and recrystallization in the weld region resulted in a significant drop in hardness relative to the surrounding base metal.

Tensile tests of the inertia friction welds in Type 303S stainless steel resulted in failure in the weld region with little ductility. At low magnification the fracture surface exhibited a spiral pattern representing a "fingerprint" of the metal flow along the weld interface. At high magnification, the fracture exhibited a "woody" appearance with thin, lenticular sulfide particles coating the surface. The orientation and shape of the sulfide particles result from the severe thermomechanical deformation which occurs during the inertia friction welding process.

Acknowledgment

This work was supported by the U.S. Department of Energy, DOE, under Contract Number DE-AC04-76DP00789.

References

1. Oberle, T. L. 1970. Inertia welding. *Metal Construction* 2(5):193-195.
2. Wang, K. K., and Wen Lin. 1974. Flywheel friction welding research. *Welding Journal* 53(6):233-s to 241-s.
3. Anon. 1979. Inertia welding: simple in principle and application. *Welding and Metal Fabrication* 47(8):585-590.
4. Wang, K. K. 1975 (April). *Friction welding.* Welding Research Council bulletin no. 204.
5. Kiwalle, J. 1967. Flywheel friction welding as a design and production tool. ASTME paper no. AD57-198.
6. Cheng, C. J. 1962. Transient temperature distribution during friction welding of two similar materials in tubular form. *Welding* Journal 41(12):542-s to 550-s.
7. Cheng, C. J. 1963. Transient temperature distribution during friction welding of two dissimilar materials in tubular form. *Welding Journal* 42(5):233-s to 240-s.
8. Wang, K. K., and Nagappan, P. 1970. Transient temperature distribution in inertia welding of steels. *Welding Journal* 49(9):419-s to 426-s.